

Effect of unusual dust event on meteorological parameters & aerosol optical and radiative properties

V. K. SONI, SANJAY BIST, R. BHATLA*, S. C. BHAN, GAJENDRA KUMAR,

M. SATEESH, SIDDHARTHA SINGH and D. R. PATTANAIK

India Meteorological Department, New Delhi – 110 003, India

**Department of Geophysics, Banaras Hindu University, Varanasi, India*

(Received 4 April 2016, Accepted 27 February 2018)

e mail : soni_vk@yahoo.com

सार - अरबी प्रायद्वीप और दक्षिणी पश्चिमी एशिया पर धूल भरी आंधी की गतिविधियों से उत्पन्न एक बहुत ही असामान्य धूल की सतह ने मार्च 20 और 23 मार्च, 2012 के बीच भारत के उत्तरी पश्चिमी क्षेत्र को प्रभावित किया जिसके कारण हवा की गुणवत्ता में महत्वपूर्ण गिरावट आई और इसके परिणामस्वरूप मौसम प्राचलों में परिवर्तन आया। 500 एनएम पर एरोसोल की ऑप्टिकल गहराई की सतह पर आधारित माप 1.015 ± 0.24 और जोधपुर में 0.837 ± 0.042 तक पहुंच गई जबकि एंगस्ट्रॉम एक्सपोनेंट क्रमशः 20 मार्च और 21 मार्च 2012 को क्रमशः -0.030 और -0.065 तक गिरा था। एओडी दिल्ली में 0.959 पर पहुंच गया जबकि एंगस्ट्रॉम एक्सपोनेंट 21 मार्च, 2012 को 0.006 पर पहुंच गया। पीएम10 की सांद्रता दिल्ली में 20 मार्च, 2012 को धूल भारी आंधी के घंटों के दौरान $1800 \mu\text{g}\text{m}^{-3}$ से अधिक असामान्य रूप से उच्च मान पर रहा। मध्यम विभेदन इमेजिंग स्पेक्ट्रोमीटर (MODIS) ने एरोसोल ऑप्टिकल गहराई को पुनः प्राप्त किया और धूल भरी आंधी और धूल की सतह के रास्ते के साथ-साथ उच्च मानों का भी प्रदर्शन किया। धूल की सतह की तीव्रता ऐसी थी कि सतह पर काफी ठंडी हो गई। सतह के स्तर पर विकिरण प्रवाह में बड़ी कमी से सतह तापमान में लगभग 2-10 डिग्री सेल्सियस तक गिरावट आई थी। शॉर्टवेव और लॉन्गवेव डायरेक्ट एयरोसोल रेडिएटिव फोर्सिंग की गणना धूल अवधि के दौरान एसबीडीएआरटी द्वारा की गई थी।

ABSTRACT. A very unusual dust plume generated from dust-storm activities over the Arabian Peninsula and Southwest Asia affected the north-west region of India between March 20 and 23, 2012, causing significant reductions in air quality and consequently changes in meteorological parameters. Ground based measurements of aerosol optical depth at 500 nm reached 1.015 ± 0.24 and 0.837 ± 0.042 at Jodhpur while Angstrom exponent dropped to -0.030 and -0.065 on March 20 and 21, 2012 respectively. The AOD reached 0.959 in Delhi while Angstrom exponent dropped to 0.006 on March 21, 2012. PM10 concentration peaked at an unusually high value of more than $1800 \mu\text{g}\text{m}^{-3}$ during dust storm hours of March 20, 2012 at Delhi. Moderate Resolution Imaging Spectrometer (MODIS) retrieved aerosol optical depth also exhibited high values as well along the path of dust storm and dust plume. The intensity of the dust plume was such that it caused significant cooling at the surface. The large reduction in the radiative flux at the surface level had caused a drop in surface temperature by approximately 2-10 °C. Shortwave and longwave Direct Aerosol Radiative Forcing was calculated using SBDART during the dust period.

Key words – Dust plume, Aerosol optical properties, Solar radiation, Radiative forcing.

1. Introduction

Dust Storms are meteorological phenomena prevalent in arid and semiarid areas, especially in tropical and subtropical latitudes. Dust storms or sand storms are more frequent during the premonsoon season in northwestern part of the Indian subcontinent adjacent to the Thar Desert, which is a primary source of dust storms in south Asia. The desert dust particles can be transported downwind depending on meteorological conditions affecting regions, hundreds of kilometers away from the source. The Indian region is also influenced by long-range dust transport from the Arabian Peninsula. Dust aerosols

have considerable impacts on human and veterinary health, ambient air quality, transport sector, weather and climate, nutrient dynamics and biogeochemical cycles of oceans and soil characteristics. The main effect of dust storms on the weather are wind shift, reduced visibility, change in humidity and temperature. Often the air ahead of a dust storm becomes extremely hot. While the temperature drops several degrees behind the leading edge of the dust storm.

Ultraviolet radiation absorbing aerosols such as mineral dust and soot cause reduction in the photolysis rate, inhibiting the ozone and smog production

(Dickerson *et al.*, 1997). The satellite measurements and surface observations have shown that the global sources of natural airborne dust particles are arid and semiarid regions contributing to the long-range transport of dust particles (Prospero, 1999; Prospero *et al.*, 2002; Washington *et al.*, 2003). Asian dust is the second largest Aeolian dust source on Earth after the Sahara dust (Tanaka and Chiba, 2006). The frequency of dust storms is closely related to local climatic conditions and surface characteristics such as vegetation cover and soil texture (Nickling and Brazel, 1984). Dust is generally categorized as coarse, fine or ultra fine. Fine dust can reach deep into the sensitive regions of the respiratory tract. A dust storm is generally dominated by coarse mode particles; therefore do not pose a serious health threat to human. But people with respiratory ailments such as asthma and emphysema may be at risk.

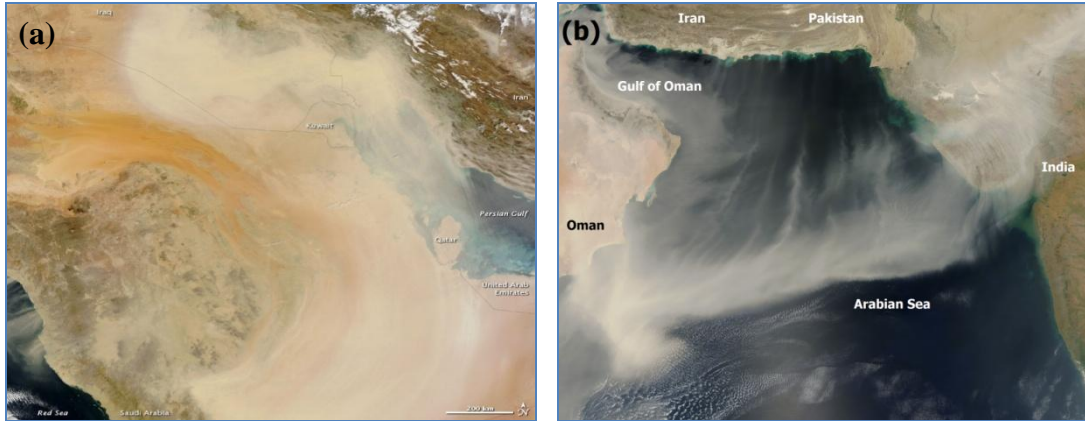
Mineral dust aerosols affect both shortwave solar and outgoing longwave radiation. Therefore, dust aerosols are considered to be an important parameter in the Earth's radiation budget studies (Satheesh and Ramanathan, 2000; Haywood and Boucher, 2000; Kaskaoutis *et al.*, 2008; Jayaraman *et al.*, 1998). The mineral dust is a significant contributor to the aerosol load with a strong seasonal cycle over the Indian region (Srivastava *et al.*, 2012). Srivastava *et al.* (2014) observed significant influence of dust storms as far as climatically sensitive Himalayan station at Manora Peak. The Great Indian Desert is the major source of mineral dust over parts of India. However, another source of mineral dust is long range transport from West Asia (Dey *et al.*, 2004). The optical properties of mineral dust change due to mixing with anthropogenic pollutants during the transport (Mishra *et al.*, 2008) which in turn influences the radiative properties. Absorption of shortwave and longwave radiation by dust aerosols increases the heating rate of the dust layer. The mixed aerosols, which consist of mineral dust and other particles, may have higher or lower absorption properties depending on the mixing of dust with soot or sulphate. The scattering and absorption reduces the incoming solar radiation reaching the surface, because of which the heating rate of the atmosphere decreases below the dust layer. On the other hand, longwave radiative forcing of dust at the surface is always positive which suggests that mineral dust warms the surface during the night when it interacts with the outgoing longwave radiation (Hansell *et al.*, 2010). Mineral dust aerosols also modify the cloud radiative forcing and thereby significantly reduce the cloud cooling effect both at the surface and TOA (Santos *et al.*, 2013). The radiative forcing by greenhouse gases is quite uniform throughout the troposphere because of longer lifetime (Hansen *et al.*, 1997), while radiative forcing by dust aerosols exhibit large spatial and temporal variations due to their relatively very short lifetime. Dust

aerosols also interact with the hydrological cycle through surface radiative forcing (Rosenfeld *et al.*, 2001). The change in surface temperature due to dust not only depends on the magnitude of radiative forcing, but also upon the extent to which the dust layer is coincident with regions of deep convection (Miller and Tegen, 1998).

The effect of mineral dust aerosols on meteorological and optical properties is complex because of a large number of different types of aerosols found in the atmosphere. Therefore, it is always practical and convenient to study the properties and effect of mineral dust during major dust outbreaks. An attempt has been made to study the complete life cycle of major dust event of March, 2012 including formation, intensification, movement and plume formation by tracking it from west Asia to Indian region till its dissipation. The dust storms of this magnitude during March are very rare and this makes this dust event as unusual. This paper presents observations made during movement of the major Asian dust plume and observed in the northern part of India, significantly affecting visibility, relative humidity, solar radiation and temperature along its path. Day-to-day variations of AOD, particle size distribution and other aerosol optical properties are also presented for this unusual dust episode. The present study also analyzed the Direct Aerosol Radiative Forcing during the dust event.

2. Data and methodology

The aerosol optical properties reported in this work were derived from Prede Skyradiometer (POM-02) data. The skyradiometer at Jodhpur and Delhi are part of Skynet-India network of India Meteorological Department. The sky radiometer observes simultaneously direct and solar aureole radiance at various scattering angles from the Sun which enables estimation of optical parameters of aerosols such as aerosol optical Depth (AOD), single scattering albedo (SSA), Ångström exponent (AE), phase function, asymmetry parameter (ASY) as well as columnar size distribution of aerosols. The measured sky radiometer data have been analyzed using SKYRAD.PACK (version 4.2) software (Nakajima *et al.*, 1996) for deriving aerosol optical properties. The calibration constant deduced from Langley method can have an error of approximately 10% for a typical urban station (Shaw, 1976). Therefore, an improved Langley method of calibration based on both direct and diffuse radiation data (Nakajima *et al.*, 1996) was used in the present study. Detailed calibration and data reduction procedures for this instrument have been described elsewhere (Tanaka *et al.*, 1986; Nakajima *et al.*, 1996; Pandithurai *et al.*, 2007).



Figs. 1 (a&b). (a) Natural-color image captured by MODIS onboard NASA's Terra satellite on March 18, 2012 and (b) MODIS onboard NASA's Aqua satellite picture on March 20, 2012, showing a giant dust plume stretched across the Arabian Sea from the coast of Oman to India

The aerosol radiative forcing (ARF) at the surface and top of the atmosphere (TOA) is defined as the difference in the net solar fluxes (down minus up) with and without aerosol. This can be represented as:

$$(\Delta F)_{STOA} = [(F_{\downarrow} - F_{\uparrow})_A]_{STOA} - [(F_{\downarrow} - F_{\uparrow})_{NA}]_{STOA}$$

where, F_{NA} and F_A , respectively, correspond to the solar flux without and with aerosols and the subscripts S and TOA refer to the Earth's surface and top of the atmosphere, respectively. The arrows indicate the direction of the fluxes, *i.e.*, \downarrow downward flux and \uparrow upward flux. The difference between the radiative forcing at the TOA and at the surface defines the atmospheric radiative forcing. Daily mean values of the ARF at the surface and TOA are derived from integration of the instantaneous ARF at the surface and TOA, averaged over 24 hours.

The net flux was computed in the short wavelength range 0.3-4.0 μm and long wavelength range 4.0 to 50.0 μm with and without aerosols at the TOA and at the surface using SBDART model. The details of SBDART model can be found in Ricchiuzzi *et al.* (1998). Based on the prevailing weather conditions and measured parameters, tropical model atmosphere was used. The ARF calculations were performed using eight radiation streams at half hour intervals for a range of solar zenith angles over a 24 hour period. The measured spectral AOD, SSA and ASY from the Skyradiometer were used for the estimation of ARF. The atmospheric heating rate due to aerosols was computed for each layer, based on finite difference estimates of the irradiance divergence at each pair of levels.

To analyze the synoptic circulation over the west and south Asia during the period of study, the mean sea level

pressure, wind fields and relative humidity were investigated using a daily NCEP Reanalysis database provided by the NOAA (website at <http://nomads.ncep.noaa.gov>). Daily maximum and minimum temperature of surface observatories obtained from India Meteorological Department were also analyzed for the Indian region.

3. Results and discussion

3.1. Genesis and movement of dust storm

Moderate Resolution Imaging Spectroradiometer (MODIS) onboard NASA's Terra satellite showed the dust blowing eastward across Iraq and its curving towards the south and southwest over Saudi Arabia on March 18, 2012 [Fig. 1(a)]. The thick dust was also observed over the westernmost point of Iran and part of the Persian Gulf. In a separate dust storm, plumes also blew westward from Saudi Arabia across the Red Sea. MODIS on-board NASA's Aqua satellite [Fig. 1(b)] showed large-scale dust plumes moving from south Oman coast to the west coast of India across the Arabian Sea on March 20, 2012. This widespread dust plume followed days of dust-storm activity over the Arabian Peninsula and Southwest Asia. The dust storm resulted from the convergence of two different weather fronts. While the first front carried dust from Iraq and Kuwait, the second front moved the dust in southeastern Iran. The low pressure area causing storm moved eastward, reaching over southeastern Iran and raised dust and sand that engulfed the northern region of the UAE, parts of Oman and the western coastal areas of Pakistan up to Karachi. This cross-continental advection of dust plumes could be due to strong subsidence with anti-cyclonic circulation over the Oman region with elongated strong ridge line almost running coincidentally with the line of dust plumes.

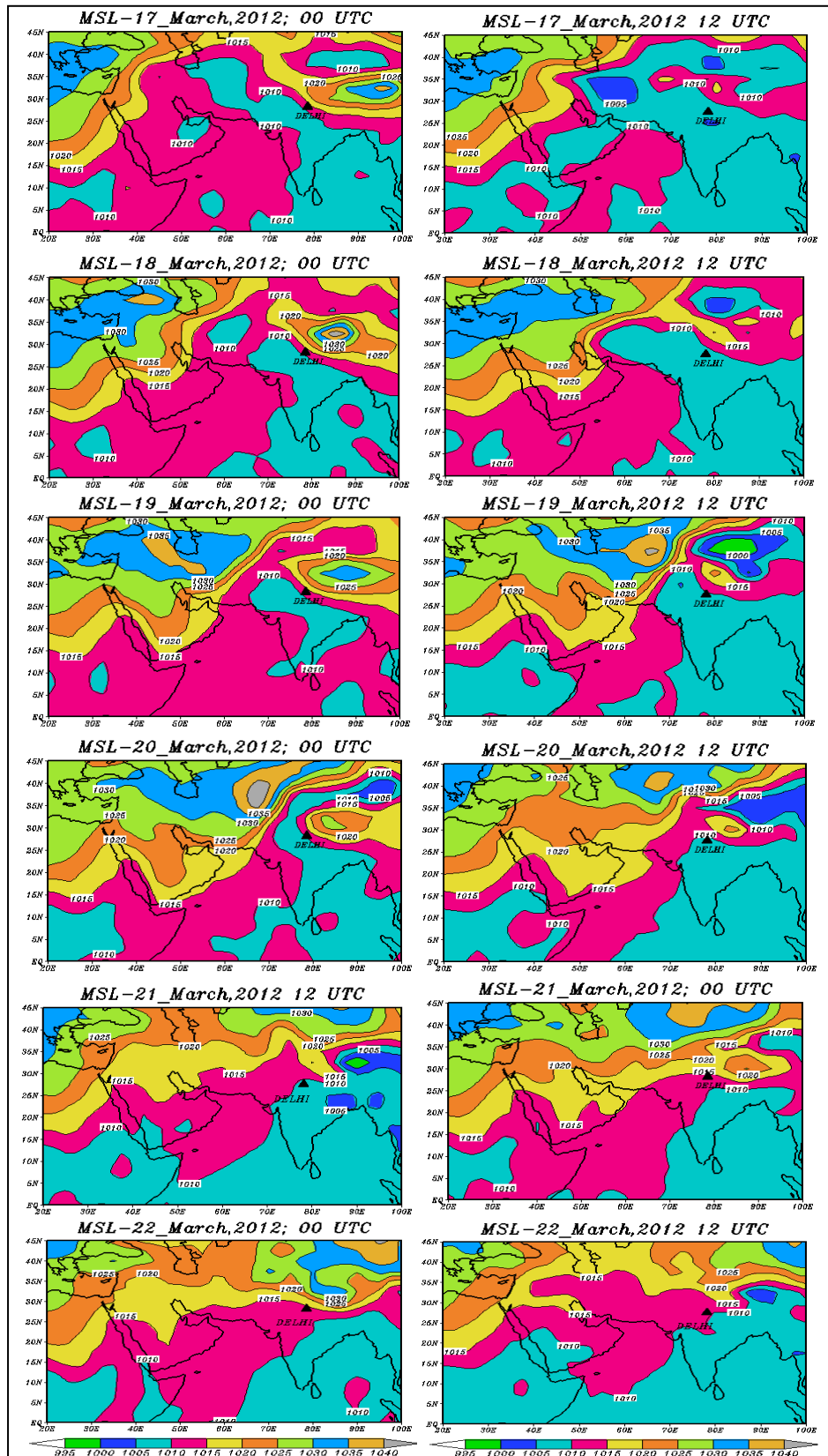


Fig. 2. Mean sea level pressure (hPa) over west and south Asia March 17, 2012 at 0000 UTC to March 22, 2012 at 1200 UTC

Fig. 2 presents the analysis of isobars at mean sea level pressure over the West and South Asia for March 17-22, 2012. On March 17, 2012, a low pressure formed over northern Iraq and winds blowing from eastern Syria to Iraq quickly accelerated towards the center of the low pressure zone. This led to the formation of a sandstorm, covering the entire land of Iraq. A high pressure with cold air formed behind the low pressure area, ensuring the movement of dust southeastward into Arabia. The duststorm then quickly engulfed Kuwait and Saudi Arabia. Later, dusty conditions made their way to Bahrain and Qatar with gusty winds. Dusty air reached over United Arab Emirates (UAE) on March 18, but with much less intensity. The high pressure area caused the dusty air to turn clockwise into central Saudi Arabia and then reaching over Yemen. A large pressure gradient set over the south-east Iran and south-west Pakistan on March 19, resulting in another massive dust storm. The sand and dust moved southward towards the north-eastern coastlines of the UAE and northern coastlines of Oman. This was incredibly rare as it is not a typical area for such large scale dust storm activity. Dusty conditions affected large parts of the Oman with visibility reducing below 500 m. Two strong pressure gradients were observed on March 19 viz., One between central Afghanistan to Rajasthan and the other between Central Arabian Sea to the west-Rajasthan with two low pressure areas formed over North Rajasthan and Oman respectively. Both the low pressure areas were of high intensity during 19-20 March causing strong pressure gradient force of 36 and 28 hPa on March 19, 2012. This unusual dust event was observed in the form of a continuous large-scale elongated plume on March 20, transporting dust towards the west coast of India. The high pressure gradients weakened considerably with flat isobars on March 21 and March 22. These dust veils were lifted from most of the land region by March 22 while it was continuing over Arabian Sea.

3.2. Wind circulation pattern

Fig. 3 illustrates the wind and relative humidity patterns at 925 hpa derived from NCEP/NCAR reanalysis from March 17 to March 22, 2012. Wind direction was northwesterly or westerly over west of 65° E and north of 25° N up to the Arabian Sea due to movement of westerly trough/Western Disturbance at 0000 UTC on March 19. Strong winds of about 40 knots in the lower tropospheric levels over west Afghanistan were observed. At 1200 UTC on March 19, northerly winds further strengthened to 50 knots and extending southwards to south of Pakistan and adjoining Arabian Sea up to Oman coast. Northerly winds of more than 50 knots were experienced over south Iran and adjoining Pakistan coasts. The dust blowing to Oman was further compounded with northwesterly winds from Iraq, adding more dust to already existing severe

dust storm. The wind circulation pattern at 925 hpa depicts that a line of subsidence or ridge line was formed at 0000 UTC on March 20 from southern Iran to the west coast of India which further strengthened till March 22. But its eastern parts gradually shifted southwards with the establishment of a strong anticyclone over Oman coast. The observations showed the vertical extent of the dust up to 8 km (Basha *et al.*, 2015).

3.3. Effect of dust plume on particulate matter

Dust storms are the result of turbulent winds, which raise large quantities of dust from desert surfaces and reduce visibility to less than 1 km. The dust concentration reaches in excess of 6000 $\mu\text{g}/\text{m}^3$ during severe dust events (Song *et al.*, 2007). The System for Air Quality Forecasting and Research which records air quality at ten stations in Delhi observed significantly high levels of both PM_{2.5} and PM₁₀. Hourly values of PM_{2.5} and PM₁₀ averaged over all the ten stations in Delhi are presented in Fig. 4. A sharp increase in the levels of PM₁₀ and PM_{2.5} was seen from around 0530 UTC. The levels of particulate matter were 8 to 10 times more on March 20 compared to that on March 19. Hourly mean value of PM₁₀ concentration was more than 1000 $\mu\text{g}/\text{m}^3$ from 0530 UTC on March 20 to 0530 UTC of March 21, 2012 reaching a maximum value of 1876 $\mu\text{g}/\text{m}^3$ at 1330 UTC on March 20. Hourly mean value of PM_{2.5} concentration was more than 250 $\mu\text{g}/\text{m}^3$ from 0530 UTC on March 20 to 0530 UTC on March 21, 2012 reaching a maximum value of 730 $\mu\text{g}/\text{m}^3$ on March 20.

3.4. Changes in aerosol optical characteristics due to dust event and aerosol radiative forcing

3.4.1. Aerosol optical depth, ångström exponent and single scattering albedo

The effect of dust plume at Jodhpur and New Delhi sites was clearly discernible through high AOD and low AE values. The AOD is representative of the airborne aerosol loading in the atmospheric column and is important for the identification of aerosol source regions and their evolution. The AE is inversely related to the average size of the particles in the aerosol, *i.e.*, smaller the particles, larger the exponent. Higher AE indicate smaller aerosol particles and vice versa. AE values generally range from greater than 2.0 for particles near combustion sources to values close to zero for coarse-mode-dominated desert dust aerosols.

The AOD values were 2 to 3 fold larger on the days of dust event than on non-dusty days in Jodhpur. In general, AOD values decrease as the wavelength increases. During the dust event, the AOD showed a trend

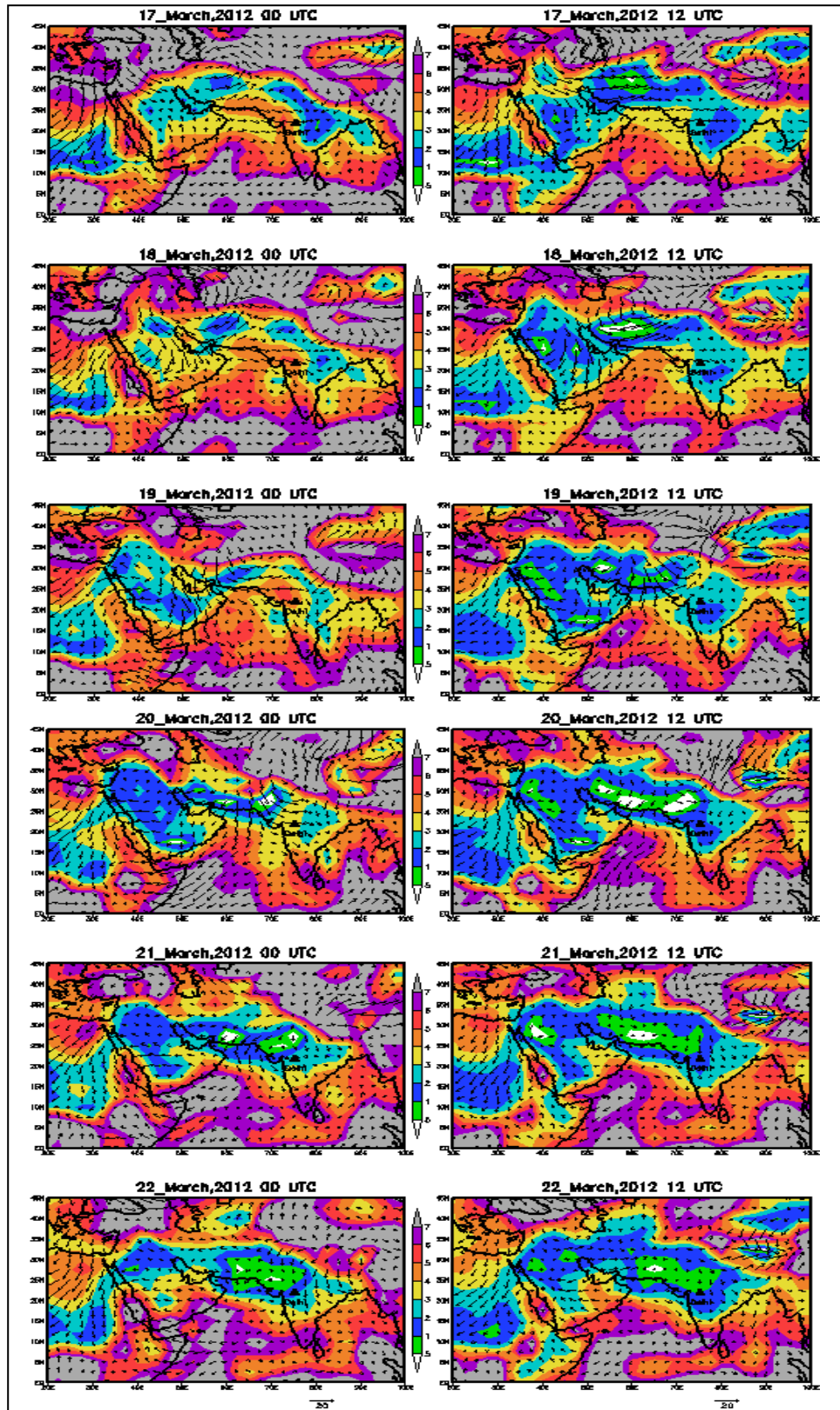


Fig. 3. Wind pattern, wind speed (m/s) and relative humidity (%) at 925 hPa (300 masl) over west and south Asia from March 17, 2012 at 0000 UTC to March 22, 2012 at 1200 UTC. RH is shown in different colours

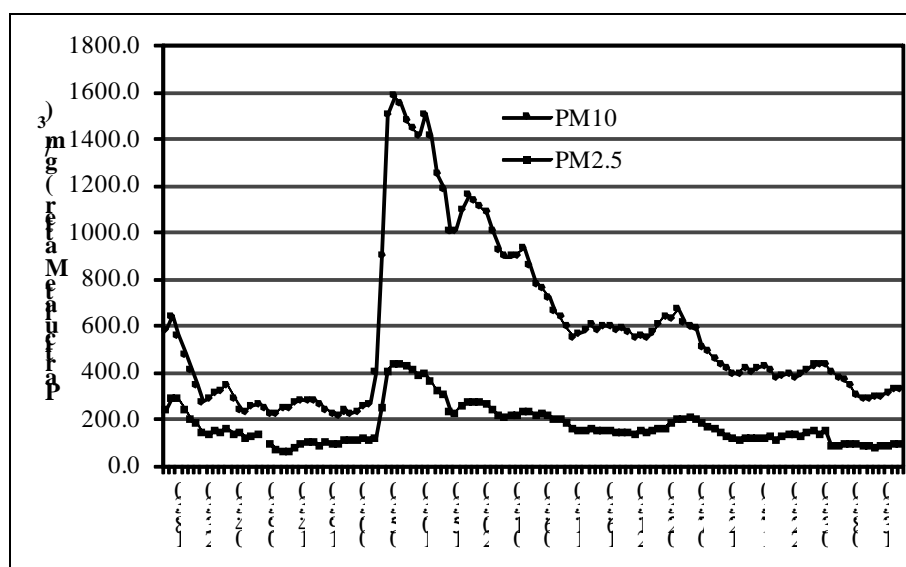


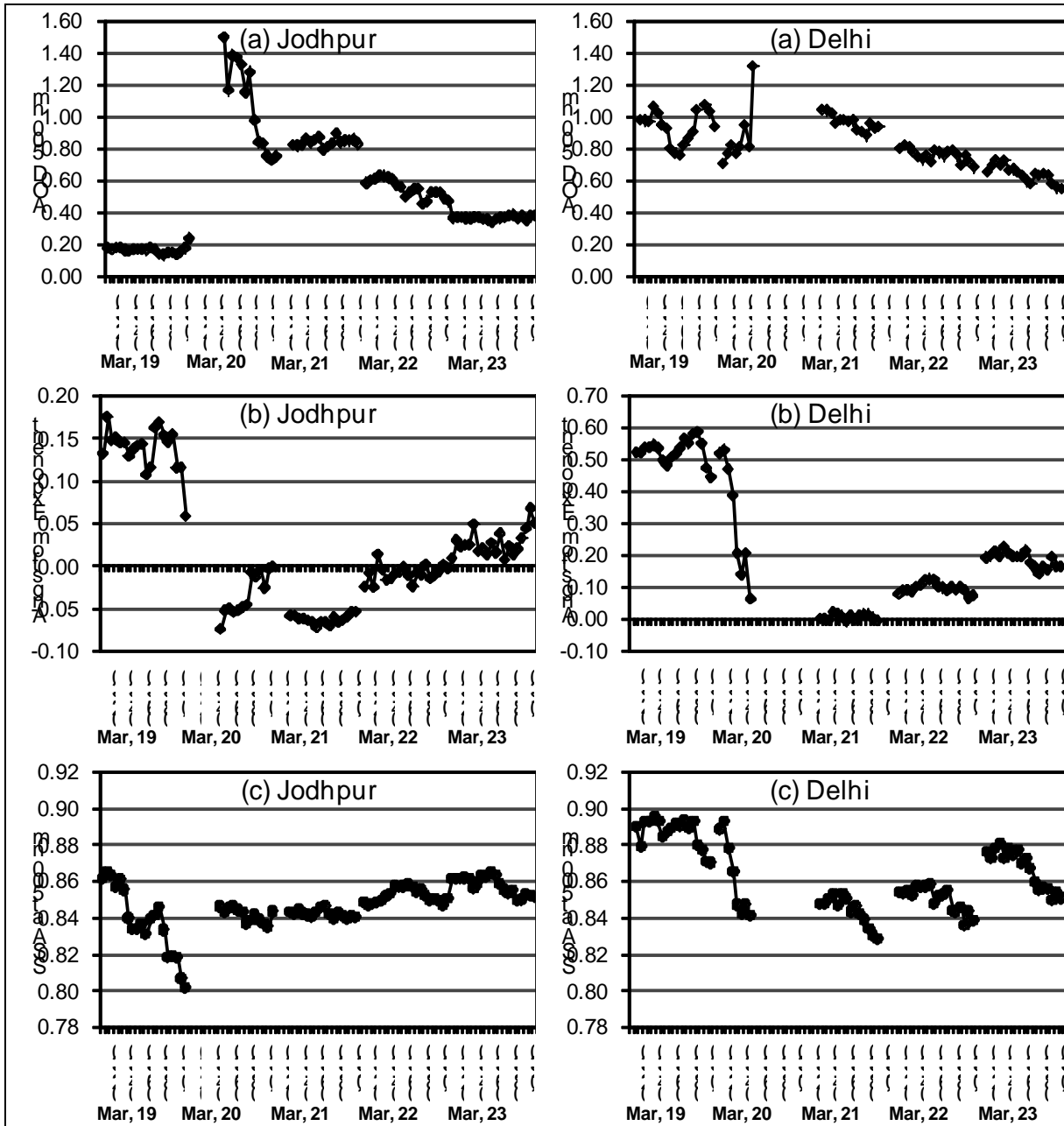
Fig. 4. Hourly mean concentration of PM10 and PM2.5 averaged over ten different locations in Delhi from March 19 to 23 March, 2012

reversal in which AOD increased with wavelength. This is an indication of the presence of higher concentration of larger particles compared to smaller particles during the dust event. Fig. 5(a) shows the half-hourly variations of the AOD at 500 nm for the five days of the study period. On March 19, the average daily AOD was around 0.17 ± 0.03 at Jodhpur. The AOD values were not available before 0530 UTC because of heavy dust loading after arrival of dust plume. In fact, significant decline was observed in direct beam irradiance since early morning associated with the arrival of dust plume at Jodhpur. The AOD value of 1.5 and AE of -0.076 was observed around 0530 UTC on March 20, indicating the increased aerosol loading in the atmosphere associated with the dust plume. AOD values remained high for the next four hours and then decreased gradually to reach a value of 0.723 by the end of the day with average daily AOD of 1.015 ± 0.24 and average AE of -0.03. Daily average value of AOD 0.837 ± 0.042 and AE value of -0.065 ± 0.01 was observed on March 21, 2012. The increase in average AOD was accompanied by a similar increase in the standard deviation, indicating greater variability in the atmospheric aerosol loading during that day. For example, the standard deviation during the day of the dust event was 0.24 at 500 nm compared with 0.03 on the preceding day. This large variability can be related to the properties of the air mass transporting the aerosols into the region.

On March 19, the average daily AOD value of 0.95 was observed in Delhi, which was higher as compared to Jodhpur. The aerosol optical properties data are not available from 0540 UTC onwards on March 20 after the

arrival of the dust plume at Delhi. The maximum AOD value of 1.49 and lowest AE value of 0.02 was observed at 0530 UTC indicating the increased aerosol loading associated with the arrival of dust plume. The significant decline was also observed in direct beam irradiance observed after 0530 UTC associated with the arrival of the dust plume at Delhi. The arrival of dust plume can also be confirmed from the sudden rise of particulate matter concentration (PM10 and PM2.5) around the same time. The AOD value at 500 nm on March 21 ranged from 1.07 to 0.87 with an average value of 0.96 ± 0.05 , while average AE was 0.006 ± 0.01 . Fig. 5(b) illustrates the time series of half hour average AE. The AE values close to zero were observed during the dust event on March 20, indicating the dominance of coarse mode particles. Low values of AE during the dust episode in March indicated that the prevailing aerosol types are clearly dust particles.

The Delhi region is known as one of the world's highly polluted urbanized areas. Biomass burning, vehicular emissions, thermal power plants and industrial units in and surrounding region are the major polluting sources (NEERI, 2010). Dust particles coated with other pollutants can have significantly different properties from those that are evident at the time of the major dust event. The scattering and absorbing nature of dust particles can be altered in different ways depending on the species coated on them (Moorthy *et al.*, 2007). Aerosols can scatter and absorb short-wave and infrared radiation in the atmosphere. The scattering versus absorption properties of an aerosol are measured by the value of the Single Scattering Albedo (SSA). SSA defined as the fraction of



Figs. 5(a-c). Half hourly values of aerosol parameters at Jodhpur and Delhi from March 19 to March 23, 2012 (a) AOD at 500 nm (b) AE and (c) SSA at 500 nm

scattering in the total extinction is a key optical characteristic in assessing the radiative effects of aerosols. The SSA depends on the aerosol size distribution, chemical composition and wavelength. The values of the SSA range from 1.0 for non-absorbing particles (perfectly white object) to zero for a perfectly black object. The absorbing feature of dust is characterized by the SSA, with low value representing high absorption. The sign at

the TOA ARF can change depending on the value of aerosol SSA (Takemura *et al.*, 2002). The time series of half hour average SSA at 500nm are depicted in Fig. 5(c) SSA at 500 nm varied between 0.86 and 0.90 with an average value about 0.88 before the dust event. On March 21, the SSA decreased to 0.82. Also, the SSA was found to increase with wavelength mainly owing to the abundance of coarse mode particles. The SSA increases

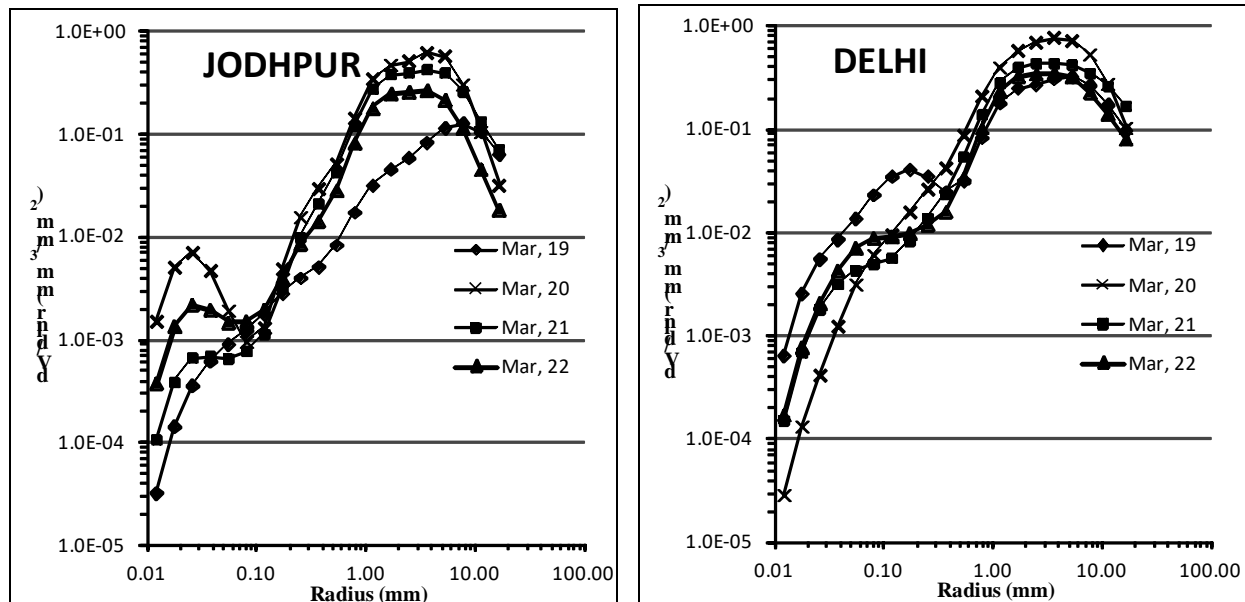


Fig. 6. Sun-skyradiometer derived mean aerosol volume size distribution at Jodhpur and New Delhi clear sky day of March 19, 2012 and on dust plume affected days from March 20 to March 22, 2012

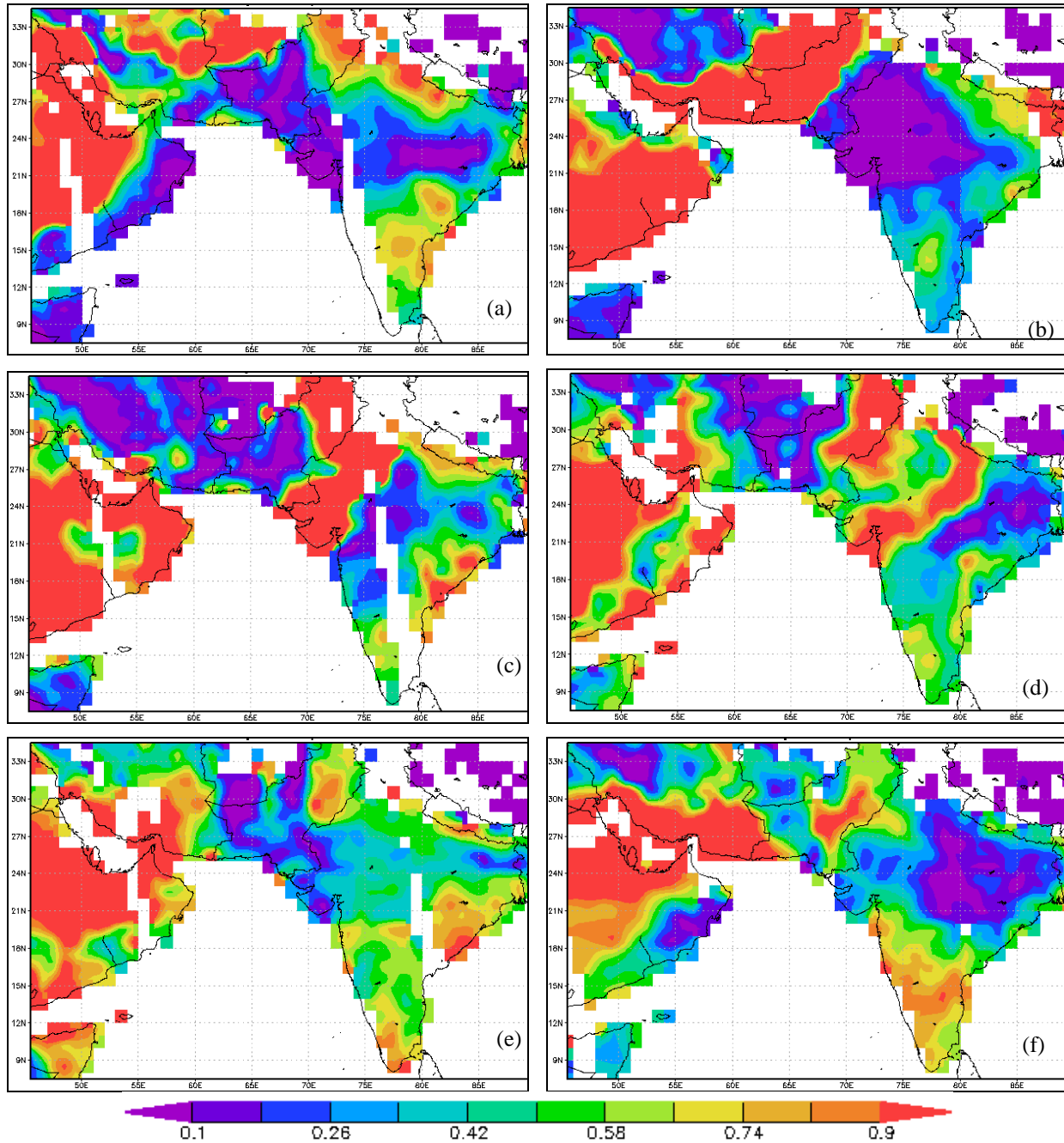
rapidly with wavelength on the dusty days as compared to non-dusty days. This rapid increase in SSA with wavelength revealed that coarse mode dust particles were dominant.

3.4.2. Volume size distribution of aerosol during dust event

The volume size distribution was retrieved from the direct solar and diffuse sky radiance measurements as discussed by Nakajima *et al.* (1996). Fig. 6 shows the ensemble of daily average aerosol volume size distribution retrieved from the sun/sky radiance data for clear sky day of March 19, 2012 at Jodhpur and Delhi and on dust affected days from March 20 to March 22, 2012. It can be seen that the aerosol distribution is bimodal with fine-particle mode around 0.1-0.2 μm and coarse particle mode around 3-4 μm . The skyradiometer observations are not available after 0540 UTC on March 20, 2012 as the sun obscured completely at Delhi because of the dust plume. Similarly, skyradiometer observations are not available before 0530 UTC on March 20 at Jodhpur because of very high dust load in the atmosphere. The volume of coarse-particle fraction was much higher on March 20-22 as compared to March 19. In strong contrast to aerosols from biomass burning and urban aerosols dominated by fine mode, dust predominantly coarse mode particles are composed of airborne desert soil minerals. The coarse mode fraction as well as fine mode fraction was significantly higher after the arrival of the dust plume.

3.4.3. MODIS aerosol optical depth at 550 nm during dust event

Fig. 7 demonstrates the spatial distribution of Aqua-MODIS AOD at 550 nm over the west and south Asia during the movement of the most intense dust plume from March 18 to March 23, 2012. MODIS AOD at 550 nm was derived using the Deep Blue algorithm (Hsu *et al.*, 2006) from MODIS-Aqua collection 5.1 (<http://disc.sci.gsfc.nasa.gov/giovanni>). The nominal equatorial passing time of Aqua satellite is around 0800 UTC. High AOD values of more than 0.9 were observed over Saudi Arabia and Iraq and also over northern parts of Iran and Afghanistan on March 18. Higher AOD values covered Saudi Arabia, Oman, Yemen, Pakistan, Afghanistan and southern parts of Iran on March 19. The AOD values were low to moderate over Indian region on March 18 and March 19. The high AOD started covering a large area over northern India from March 20. During the intense dust episode, AOD values of more than 0.9 were observed over north-western and northern part, namely Gujarat, Rajasthan and Punjab, indicating enhanced presence of dust aerosols. The region of higher AOD shifted southward on March 21. This is suggested in combination with the extremely high AOD and the air-mass trajectories (not shown here) revealing origin from the desert and arid regions of southwest Asia. High values of AOD were still observed over parts of the Arabian Peninsula while AOD values reduced significantly over Indian region on March 22 and March 23, 2012.



Figs. 7(a-f). AQUA-MODIS (Deep Blue) AOD distribution over west & south Asia on (a) 18, (b) 19, (c) 20, (d) 21, (e) 22 and (f) 23 March, 2012

3.4.4. Effect of dust event on solar radiation and radiative forcing

The long range transport of dust during a sand-dust storm plays an important role in the Earth-atmosphere system. Dust aerosols in the atmosphere redistribute radiative heating at the surface and in the atmosphere by scattering & absorbing shortwave radiation. Dust aerosols also scatter, absorb and emit infrared radiation. Radiative

impact of aerosols depends on aerosol concentration, size and chemical composition. A negative value of TOA ARF leads to cooling of the Earth-atmosphere system because of backscattering by aerosols, while positive radiative forcing implying warming of the atmosphere. Radiative effects of dust aerosols are also a function of dust layer height (Zhu *et al.*, 2007; Forster *et al.*, 2007). The low level dust layer induces small cooling at the surface, while an elevated dust layer and a uniform distribution of dust

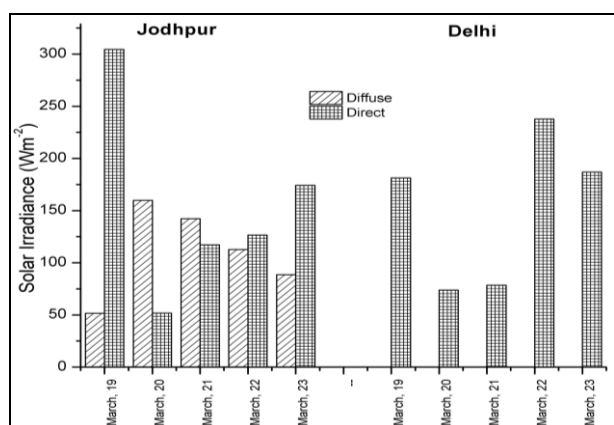


Fig. 8. Variation of diffuse and direct solar irradiance during dust event at Jodhpur and Delhi

aerosols can cause large surface cooling (Chung & Zhang, 2004). In case of low-level dust layer, vertical mixing and turbulent fluxes partially balance the surface cooling by transferring the absorbed heat from the dust layer downward to the surface. On the other hand, there is little transfer of absorbed heat from the elevated dust layer to the surface as the heating occurs well above the planetary boundary layer (Chung and Zhang, 2004). Zhu *et al.* (2007) found that dust plumes over Arabian Sea have the largest effect on atmospheric heating when compared with Yellow Sea and Saharan coast because of lower SSA and the relatively large dust loading. They observed that maximum shortwave heating occurs over Arabian Sea with the value around +0.5 K/day inside the dust layer at about 4 km height where dust concentration peaks.

The reduction of solar radiation at the surface during the dust event of March 2012 is shown in Fig. 8. Direct irradiance showed a very unusual and strong attenuation, reducing to 50.5 Wm^{-2} on March 20 as compared with 304.5 Wm^{-2} on March 19, the day before the dust plume reached Jodhpur while diffuse irradiance increased from 51.6 Wm^{-2} on March 19 to 159.9 Wm^{-2} on March 20. The daily mean direct solar irradiance value of 181.4 Wm^{-2} was observed on March 19 which reduced to 73.8 Wm^{-2} on March 20 and remained 78.5 Wm^{-2} on March 21, 2012. The daily mean direct solar irradiance value increased to 237.8 Wm^{-2} on March 22.

Pandithurai *et al.* (2008) estimated DARF during premonsoon season of 2006 over Delhi suggesting a consistent increase in cooling of surface from -39 Wm^{-2} in March to -99 Wm^{-2} in June, while the atmospheric the lower atmosphere. In addition, values of forcing heating ranged from $+27 \text{ Wm}^{-2}$ (March) to $+123 \text{ Wm}^{-2}$ (June) since dust events lead to enhanced heating rates in efficiency at the surface were found to be -71 , -85 , -87 and -84 Wm^{-2} for March, April, May and June 2006,

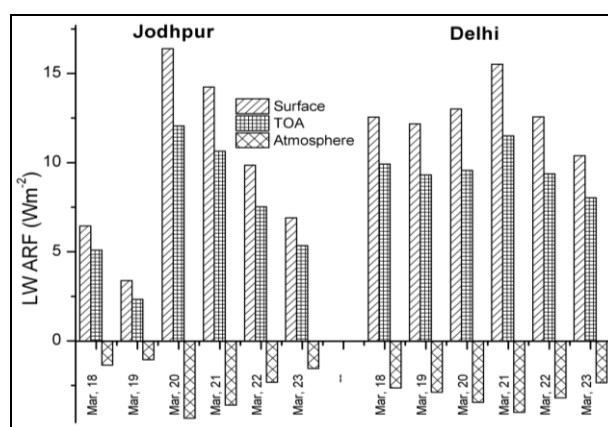
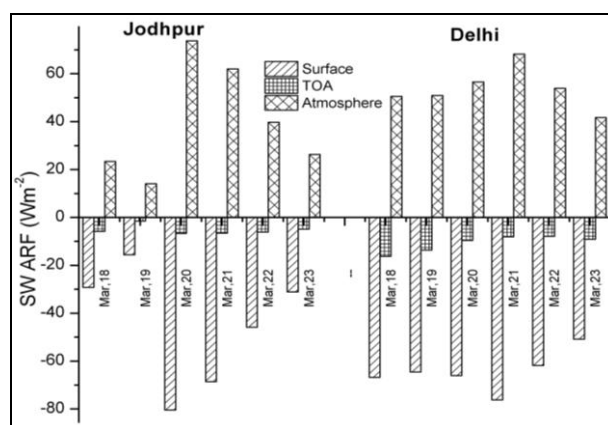


Fig. 9. Variation of SW and LW Direct aerosol radiative forcing at surface, TOA and atmosphere during dust event from March 18 to March 23, 2012 observed at Jodhpur and Delhi

respectively. These larger forcing efficiency values compared to other stations indicate more absorbing nature of aerosols over urban Delhi. Prasad *et al.* (2007) reported the surface and TOA forcing in the range of -19 to -87 Wm^{-2} and $+2$ to -26 Wm^{-2} respectively, during the dust period from April-May, 2005.

The daily shortwave (SW) and Longwave (LW) aerosol radiative forcing results are shown in Fig. 9. The average daily AOD at 500 nm was 0.168, 1.015, 0.837, 0.546 and 0.364 while SSA was 0.869, 0.837, 0.840, 0.842, 0.852 and 0.857 from March 19 to March 23 respectively at Jodhpur. The estimated daily SW ARF at the surface was -15.5 , -69 , -65.2 , -47.3 and -30.7 Wm^{-2} for March 19 to March 23, 2012 respectively. Forcing values at the TOA were -1.9 , $+2.6$, -6.3 , -6.0 and -6.4 Wm^{-2} and hence the atmospheric forcing values are $+13.6$, $+71.6$, $+58.9$, $+41.2$ and $+24.3 \text{ Wm}^{-2}$ for March 19 to March 23, 2012 respectively at Jodhpur. Higher surface aerosol forcing on March 20, 2012 is due to the higher aerosol loading as the average AOD value of 1.09 was observed at 500 nm.

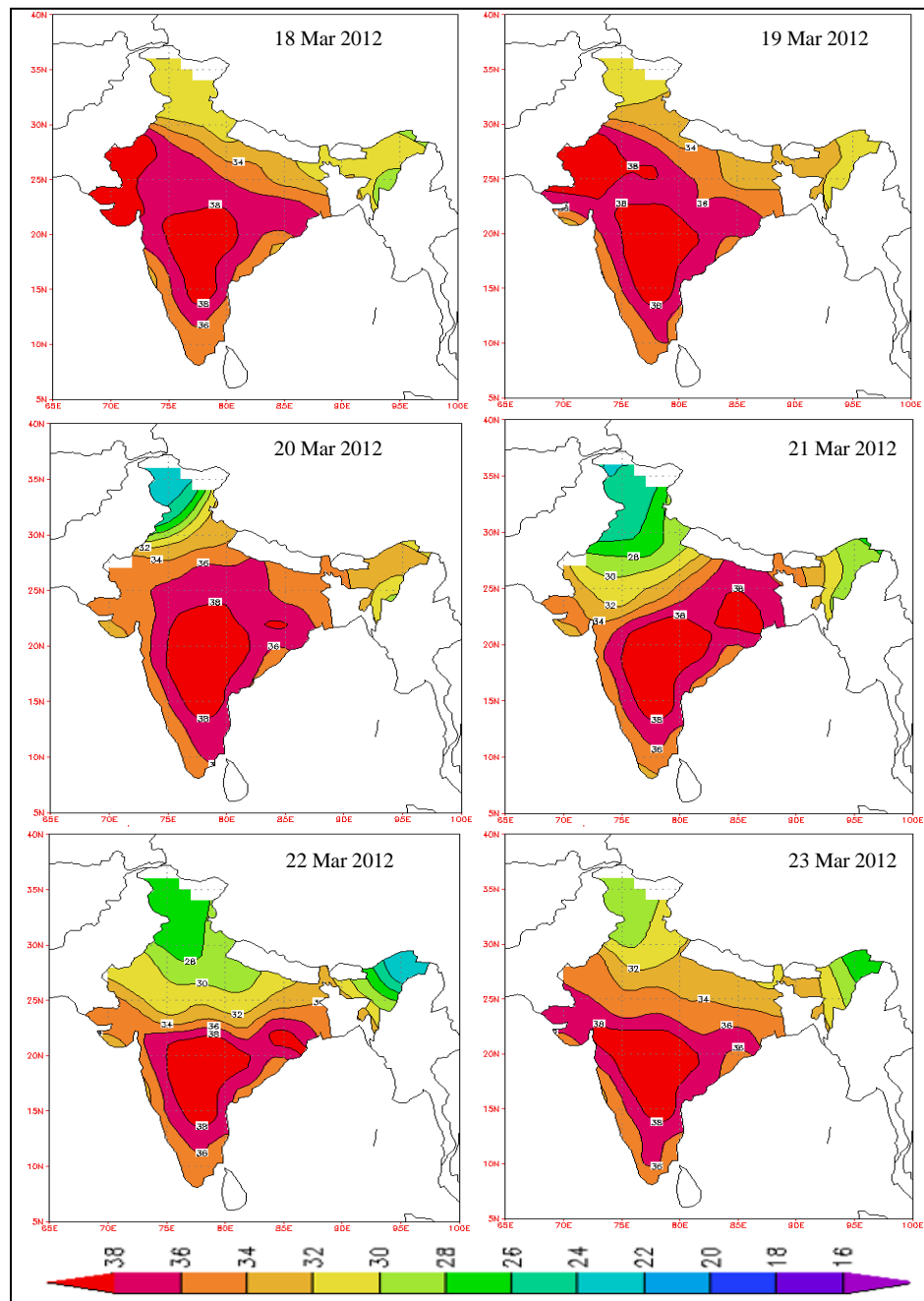


Fig. 10(a). Distribution of maximum temperature ($^{\circ}\text{C}$) before and after the dust plume over Indian region

The effect on DARF is not much pronounced in Delhi as the atmosphere was also turbid before the dust episode. The average daily AOD at 500 nm was 1.044, 0.945, 0.884, 0.956, 0.756 and 0.636 while SSA was 0.898, 0.887, 0.865, 0.844, 0.850 and 0.866 from March 18 to March 23 respectively at Delhi. The sun completely obscured on March 20 and aerosol optical properties could not be obtained because of dust plume before 0530 UTC at Jodhpur and after 0540 UTC at Delhi on March 20,

2012. Hence, skyradiometer data on March 20 are not actually representative of dust event. The estimated SW ARF at the surface was -58.2 , -50.8 , -59.5 , -57.5 and -48.5 Wm^{-2} for March 19 to March 23, 2012 respectively at Delhi. Forcing values at the TOA are -12.0 , $+4.4$, $+8.9$, -7.0 and -10.8 Wm^{-2} and hence the atmospheric forcing values are $+46.3$, $+55.3$, $+68.4$, $+50.5$ and $+37.7$ Wm^{-2} for March 19 to March 23, 2012 respectively at Delhi. In addition, the negative shortwave DARF value at the

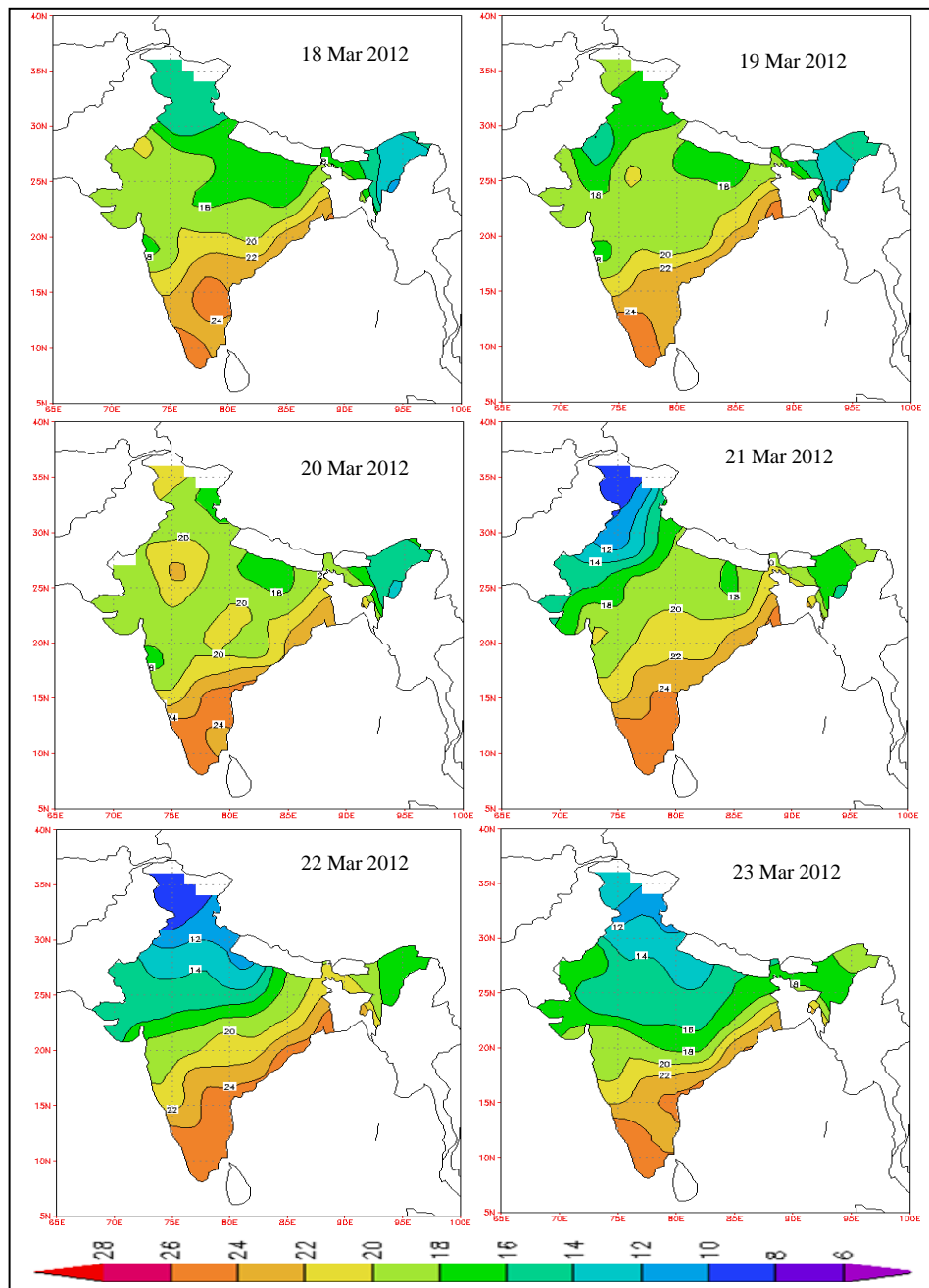


Fig. 10(b). Distribution of Minimum Temperature ($^{\circ}\text{C}$) before and after the dust plume over Indian region

surface reveals that the desert dust aerosol significantly reduced the solar radiation reaching the ground level, thus producing a large cooling effect on the surface level. This result confirms a significant absorption of solar radiation in the atmosphere, leading to considerable atmospheric warming. It is distinct that high heating rates correspond with high AOD and high shortwave DARF during the dust event in the atmosphere.

Dust can affect both the shortwave and longwave components of the radiative energy balance, but in opposing ways. In contrast to the reduction in SW radiation, dust significantly increases the LW radiation reaching the surface. Huang *et al.* (2009) found that about one third of the SW radiative cooling effect caused by Asian dust is compensated by its longwave warming effect and about two thirds of the warming effect at the TOA is related to the longwave radiation. The

corresponding average daily ARF in the LW region at the surface were 6.4, 3.4, 16.4, 14.2, 9.8 and 6.9 Wm^{-2} while at the TOA 5.1, 2.3, 12.1, 10.6, 7.5 and 5.3 Wm^{-2} for March 18 to March 23, 2012 respectively at Jodhpur. The estimated average daily LW ARF at the surface were 12.6, 12.2, 13, 15.5, 12.6 and 10.4 Wm^{-2} while at the TOA 9.9, 9.3, 9.6, 11.5, 9.4 and 8.0 Wm^{-2} for March 18 to March 23, 2012 respectively at Delhi. LW warming effects therefore compensates SW cooling at the surface & TOA.

3.5. *Effect of dust plume on meteorological parameters*

Dust over Indian region started approaching over two pockets from March 20, 2012; one over North-west India and other over Gujarat and Mumbai coast. The surface meteorological elements such as temperature, visibility and relative humidity responded significantly to the change in dust aerosol concentration. Significant negative surface forcing as explained in the previous section caused the decline in temperature during the dust events. Distribution of maximum and minimum temperature before and after the dust plume over Indian region is presented in Figs. 10(a&b). Maximum temperatures on March 19 were above normal by 4 to 7 °C over many parts of Punjab, Haryana, Rajasthan and Arunachal Pradesh & east Assam; by 2 to 3 °C over many parts of Gujarat region, central and peninsular India and remaining parts of northeastern states; below normal by 2 to 3 °C over some parts of Gangetic West Bengal and isolated pockets of Bihar and Jharkhand and near normal over rest parts of the country. Minimum temperatures were above normal by 2 to 5 °C over many parts of the western Himalayan region, Punjab, Haryana, Delhi, west Uttar Pradesh, Rajasthan and West Bengal & Sikkim and below normal by 2 to 4 °C over some parts of Konkan and northeastern states and near normal over rest parts of the country. On March 20, minimum temperature was higher by 2 to 4 °C over some parts of Jammu & Kashmir, Punjab and north Gujarat and isolated pockets of Rajasthan, Madhya Pradesh, Vidarbha and west Bengal & Sikkim. The minimum temperature was above normal by 5 to 7 °C over the western Himalayan region, Punjab, Haryana and Rajasthan and by 2 to 4 °C over parts of north Gujarat and west Madhya Pradesh. The weather remained mainly dry over most parts of the country except Jammu & Kashmir. The maximum temperatures on March 20 decreased by 5 to 10 °C over many parts of Rajasthan, some parts of Punjab and Jammu & Kashmir; by 2 to 4 °C over some parts of Himachal Pradesh, Uttarakhand, Haryana and Delhi. Maximum temperature increased by 2 to 3 °C over some parts of eastern Uttar Pradesh and isolated pockets of Bihar, Jharkhand and Gangetic West Bengal which were not affected by dust plume. The maximum temperatures were below normal by 2 to 4 °C

over some parts of west Rajasthan and Punjab; above normal by 2 to 5 °C over rest parts of the country outside Gujarat, Bihar, Jharkhand, Gangetic West Bengal, south interior Karnataka and west coast the temperature was found to be near normal.

On March 21, dust haze was prevailing over Punjab, Haryana, Delhi, Uttar Pradesh, Rajasthan, Gujarat and Madhya Pradesh. Minimum temperatures fell by 4 to 8 °C over many parts of Jammu & Kashmir, Punjab, Haryana, Delhi and Rajasthan; by 2 to 3 °C over parts of Himachal Pradesh, Uttar Pradesh, Madhya Pradesh and Gujarat. The minimum temperatures were below normal by 2 to 3 °C over the plains of northwest India. Maximum temperatures fell by 2 to 6 °C over many parts of northwest and adjoining central India and rose by 2 to 3 °C over many parts of eastern India. The maximum temperatures were below normal by 2 to 4 °C over many parts of Punjab, Haryana, Rajasthan and some parts of west Uttar Pradesh and northwest Madhya Pradesh and above normal by 2 to 4 °C over many parts of the western Himalayan region, northeast, east and north peninsular India and near normal over rest parts of the country. Dust leads to a large decrease in surface air temperature. Such a reduction is attributed to the negative short-wave dust ARF at the surface, which surpasses the warming by the thermal radiative forcing.

Before the arrival of the storm, the weather was stable with clear sky; Temperature was 26.6 °C, Pressure 1007 hPa, RH 21%, visibility 2000 m and the local wind was relatively light and westerly at 2100 UTC on March, 19, 2012 at Jodhpur. Around 0000 UTC on March 20, with the arrival of the dust plume, there were dramatic changes in visibility. The visibility reduced to 1000 m at 0000 UTC and further deteriorated to 200 m at 0600 UTC and remained 200 m till 0900 UTC. Visibility increased to 500 m at 1200 UTC and further to 1000 m at 1500 UTC. The large scale dust plume caused visibility to fall from 0600 UTC in Delhi when it suddenly fell from 3000 m to 1000 m. From changes in meteorological parameters, it is established that dust plume approached at Jodhpur around 0000 UTC and at Delhi around 0600 UTC. The lowest visibility of 200 m covered Rajasthan on March 20, 2012 and visibility of 500-1000 m covering most parts of western and North-west India. Cities like Jaipur, Jodhpur, Ahmedabad and Ludhiana had visibility of 500-800 m in the morning hours. Visibility of 4000 m was observed at Karachi Airport on March 19 at 1200 UTC which decreased significantly to 500 m at 1500 UTC and further to 200 m at 1800 UTC.

The semi-direct effect of aerosols was introduced by Hansen *et al.* (1997) to describe the impact of absorbing aerosols on clouds. A series of experiments with a simple

general circulation model showed that increased shortwave absorption could reduce relative humidity and subsequently decrease cloud cover. Ackerman *et al.* (2000) investigated the semi-direct aerosol effect and found that absorbing aerosols reduce the relative humidity in the boundary layer. Jacobson (2002) found a decrease in global averaged column liquid water and ice associated with the strong warming influence of absorbing aerosols. The dust storm events are usually associated with low relative humidity weather conditions (Ling, 2010). Relative humidity (RH) was the highest before the dust storm event, reaching a maximum of 60% on March 19 at 0000 UTC at Jodhpur. Relative humidity then dropped sharply and the respective values for March 20 at 0000 and 0600 UTC were only 18% and 4%. Dew-point depressions of 44 °C or more occurred after passage of the dust plume at Jodhpur and Karachi. RH of 56% was observed at Karachi Airport on March 19 at 1500 UTC which decreased significantly to 7% at 1800 UTC and further reduced to 2% at 0600 UTC on March 20. RH less than 10% was observed over large parts of Iran, Afghanistan, Pakistan, Saudi Arab, Oman, Yemen and northwest India during dust event on March 19 and 20 (Fig. 3). After the dust event, the relative humidity recovered gradually. Reduction of the RH was observed due to the increase in dust AOD levels. Dust aerosol impacts negatively on the atmospheric moisture levels. Significant reduction of relative humidity during the dust event can be attributed to the mixture of dry air masses associated with dust storms and the absorption of incoming solar short wave radiation by dust aerosols.

4. Conclusions

Severe dust-storm activities over the Arabian Peninsula and Southwest Asia affected the north-west region of India between March 20 and 23, 2012. The strong winds in surface and middle troposphere favored the uplift and long-range transport of desert-dust covering an extended area of the Iraq, Kuwait, Iran, UAE, Oman, Afghanistan, Pakistan and India. The dust episode was capable of reducing direct solar radiation by as much as 80% and a corresponding increase of 300% in diffuse solar irradiance during cloudless days. Ground based measurement of AOD at 500 nm reached 1.015 and 0.837 at Jodhpur while AE dropped to -0.030 and -0.065 on March 20 and 21 respectively. The average daily AOD reached 0.956 at Delhi while AE reduced to 0.006 on March 21, 2012. PM10 concentration peaked at unusually high value of more than 1800 $\mu\text{g m}^{-3}$ during dust storm hours of March 20 at Delhi. Moderate Resolution Imaging Spectrometer retrieved AOD also exhibited high values along the path of dust storm and dust plume. The estimated daily SW ARF at the surface was -80.4 and -68.6 W m^{-2} at Jodhpur and -66.1 and -76.2 W m^{-2} at Delhi

for March 20 and March 21, 2012 respectively. The net DARF was dominated by the shortwave cooling at TOA due to the backscattering of incoming solar radiation and cooling at surface level due to the attenuation of solar radiation by the dust layer. The large reduction in the radiative flux at the surface level had caused a significant drop in surface temperature by approximately 2 - 10 °C. Extremely low visibility up to 200m was observed at many sites such as Karachi, Jodhpur, Ahmedabad during the dust event. Relative humidity less than 10% was observed over large parts of Iran, Afghanistan, Pakistan, Saudi Arab, Oman, Yemen and northwest India during the dust event.

Acknowledgement

Authors are grateful to Director General of Meteorology India Meteorological Department, New Delhi for encouraging this research work. The contents and views expressed in this research paper are the views of the authors and do not necessarily reflect the views of the organizations they belong to.

References

- Ackerman, A. S., Toon, O. B., Stevens, D. E., Heymsfield, A. J., Ramanathan, V. and Welton, E. J., 2000, "Reduction of tropical cloudiness by soot", *Science*, **288**, 1042-1047.
- Basha, G., Phanikumar, D. V., Niranjan Kumar, K., Ouarda, T. B. M. J. and Marpu, P. R., 2015, "Investigation of aerosol optical, physical and radiative characteristics of a severe dust storm observed over UAE", *Remote Sensing of Environment*, **169**, 404-417.
- Chung, C. E. and Zhang, G. J., 2004, "Impact of absorbing aerosol on precipitation: dynamic aspects in association with convective available potential energy and convective parameterization closure and dependence on aerosol heating profile", *J. Geophys. Res.*, **109**, D22103. <http://dx.doi.org/10.1029/2004JD004726>.
- Dey, S., Tripathy, S. N., Kingand, R. P. and Holben, B. N., 2004, "Influence of dust storms on aerosol optical properties over the Indo-Gangetic basin", *J. Geophys. Res.*, **109**, D20211, doi: 10.1029/2004JD004924.
- Dickerson, R. R., Kondragunta, S., Stenchikov, G., Civerolo, K. L., Doddridge, B. G. and Holben, B. N., 1997, "The impact of aerosols on solar ultraviolet radiation and photochemical smog", *Science*, **278**, 827-830.
- Forster, P., Ramaswamy, V., Artaxo, P., Bernsten, T., Betts, R., Fahey, D. W., Haywood, J., Lean, J., Lowe, D. C., Myhre, G., Nganga, J., Prinn, R., Raga, G., Schulz, M. and Dorland, R. V., 2007, *In Changes in Atmospheric Constituents and in Radiative Forcing*, Cambridge University Press, Cambridge.
- Hansell, R. A., Tsay, S. C., Ji, Q., Hsu, N. C., Jeong, M. J., Wang, S. H., Reid, J. S., Liou, K. N. and Ou, S. C., 2010, "An assessment of the surface longwave direct radiative effect of airborne Saharan dust during the NAMMA field campaign", *J. Atmos. Sci.*, **67**, 1048-1065.
- Hansen, J., Sato, M. and Ruedy, R., 1997, "Radiative forcing and climate response", *J. Geophys. Res.*, **102**, 6831- 6864.

- Haywood, J. M. and Boucher, O., 2000, "Estimates of the direct and indirect radiative forcing due to tropospheric aerosols: A review", *Rev. Geophys.*, **38**, 513-543.
- Hsu, N. C., Tsay, S. C., King, M. D. and Herman, J. R., 2006, "Deep Blue retrievals of Asian aerosol properties during ACE-Asia", *IEEE T. Geosci. Remote Sens.*, **44**, 3180-3195.
- Huang, J., Fu, Q., Su, J., Tang, Q., Minnis, P., Hu, Y., Yi, Y. and Zhao, Q., 2009, "Taklimakan dust aerosol radiative heating derived from calipso observations using the Fu-Liou radiation model with Ceres constraints", *Atmos. Chem. Phys.*, **9**, 4011-4021.
- Jacobson, M. Z., 2002, "Control of fossil-fuel particulate black carbon and organic matter, possibly the most effective method of slowing global warming", *J. Geophys. Res.*, **107**, 4410, doi: 10.1029/2001JD001376.
- Jayaraman, A., Lubin, D., Ramachandran, S., Ramanathan, V., Woodbridge, E., Collins, W. D. and Zalupuri, K. S., 1998, "Direct observation of aerosol radiative forcing over the tropical Indian Ocean during the Jan.- Feb. 1996 pre-INDOEX cruise", *J. Geophys. Res.*, **103**, 13827-13836.
- Kaskaoutis, D. G., Kambezidis, H. D., Nastos, P. T. and Kosmopoulos, P. G., 2008, "Study on an intense dust storm over Greece", *Atmos. Environ.*, **42**, 6884-6896.
- Ling, X. L., Guo, W. D., Zhang, L. and Zhang, R. J., 2010, "A Case Study of the Impacts of Dust Aerosols on Surface Atmospheric Variables and Energy Budgets in a Semi-Arid Region of China", *Atmos. Oceanic Sci. Lett.*, **3**, 145-150.
- Miller, R. L. and Tegen, I., 1998, "Climate response to soil dust aerosols", *J. Clim.*, **11**, 3247-3267.
- Mishra, S. K., Dey, S. and Tripathi, S. N., 2008, "Implications of particle composition and shape to dust radiative effect: A case study from the Great Indian Desert", *Geophys. Res. Lett.*, **35**, 1-5, doi:10.1029/2008GL036058.
- Moorthy, K. K., Babu, S. S., Satheesh, S. K., Srinivasan J. and Dutt, C. B. S., 2007, "Dust absorption over the "Great Indian Desert" inferred using ground-based and satellite remote sensing", *J. Geophys. Res.*, **112**, D09206.
- Nakajima, T., Tonna, G., Rao, R., Boi, P., Kaufman, Y. and Holben, B. N., 1996, "Use of sky brightness measurements from ground for remote sensing of particulate polydispersions", *Appl. Opt.*, **35**, 2672-2686.
- NEERI, 2010, "Air Quality Monitoring, Emission Inventory & Source Apportionment Studies for Delhi. Prepared by National Environmental Engineering Research Institute, Nagpur, India", <http://www.cpcb.nic.in/Delhi.pdf>.
- Nickling, W. G. and Brazel, A. J., 1984, "Temporal and spatial characteristics of Arizona dust storms (1965-1980)", *J. Climat.*, **4**, 645-660.
- Pandithurai, G., Pinker, R. T., Devara, P. C. S., Takamura, T. and Dani, K. K., 2007, "Seasonal asymmetry in diurnal variation of aerosol optical characteristics over Pune, western India", *J. Geophys. Res.*, **112**, D08208, doi:10.1029/2006JD007803.
- Pandithurai, G., Dipu, S., Dani, K. K., Tiwari, S., Bisht, D. S., Devara, P. C. S. and Pinker, R. T., 2008, "Aerosol radiative forcing during dust events over New Delhi, India", *J. Geophys. Res.*, **113**, D13209, doi:10.1029/2008JD009804.
- Prasad, A. K., Singh, S., Chauhan, S. S., Srivastava, M. K., Singh, R. P. and Singh, R., 2007, "Aerosol radiative forcing over the Indo-Gangetic Plains during major dust storms", *Atmos. Environ.*, **41**, 6289-6301.
- Prospero, J. M., 1999, "Long-term measurements of the transport of African mineral dust to the southeastern United States: Implications for regional air quality", *J. Geophys. Res.*, **104**, 15917-15927.
- Prospero, J. M., Ginoux, P., Torres, O., Nicholson, S. E. and Gill, T. E., 2002, "Environmental characterization of global sources of atmospheric soil dust identified with the Nimbus 7 Total ozone Mapping Spectrometer (TOMS) absorbing aerosol product", *Rev. Geophys.*, **40**, 1002, doi:10.1029/2000RG000095.
- Ricchiazzi, P., Yang, S., Gautier, C. and Sowle, D., 1998, SBDART, "A research and teaching tool for plane-parallel radiative transfer in the Earth's atmosphere", *B. Am. Meteorol. Soc.*, **79**, 2101-2114.
- Rosenfeld, D., Rudich, Y. and Lahav, R., 2001, "Desert dust suppressing precipitation: A possible desertification feedback loop", *Proc. Natl. Acad. Sci. U.S.A.*, **98**, 5975-5980.
- Santos, D., Costa, M. J., Silva, A. M. and Salgado, R., 2013, "Modeling Saharan desert dust radiative effects on clouds", *Atmos. Res.*, **127**, 178-194.
- Satheesh, S. K. and Ramanathan, V., 2000, "Large differences in tropical aerosol forcing at the top of the atmosphere and Earth's surface", *Nature*, **405**, 60-63.
- Shaw, G. E., 1976, "Error analysis of multi-wavelength sunphotometry", *Pure Appl. Geophys.*, **114**, 1-14, doi:10.1007/BF00875487.
- Song, Z., Wang, J. and Wang, S., 2007, "Quantitative classification of northeast Asian dust events", *J. Geophys. Res.*, **112**, D04211, doi:10.1029/2006JD007048.
- Srivastava, A. K., Soni, V. K., Singh, S., Kanawade, V. P., Singh, N., Tiwari, S. and Attri, S. D., 2014, "An early South Asian dust storm during March 2012 and its impacts on Indian Himalayan foothills: A case study", *Science of Total Environment*, **493**, 526-534, <http://dx.doi.org/10.1016/j.scitotenv.2014.06.024>.
- Srivastava, A. K., Tripathi, S. N., Dey, S., Kanawade, V. P. and Tiwari, S., 2012, "Inferring aerosol types over the Indo-Gangetic Basin from ground-based sunphotometer measurements", *Atmos. Res.*, **109**, 64-75.
- Takemura, T., Nakajima, T., Dubovik, O., Holben, B. N. and Kinne, S., 2002, "Single scattering albedo and radiative forcing of various aerosol species with a global three dimension model", *J. Clim.*, **15**, 333-352, doi:10.1175/1520-0442.
- Tanaka, M., Nakajima, T. and Shiobara, M., 1986, "Calibration of a sun photometer by simultaneous measurements of direct-solar and circumsolar radiations", *Appl. Opt.*, **25**, 1170-1176.
- Tanaka, T. Y. and Chiba, M., 2006, "A numerical study of the contributions of dust source regions to the global dust budget", *Global Planet. Change*, **52**, 88-104.
- Washington, R., Todd, M., Middleton, N. J. and Goudie, A. S., 2003, "Dust storm source areas determined by the Total Ozone Monitoring Spectrometer and surface observations", *Ann. Assoc. Am. Geogr.*, **93**, 297-313.
- Zhu, A., Ramanathan, V., Li, F. and Kim, D., 2007, "Dust plumes over the Pacific, Indian and Atlantic oceans: Climatology and radiative impact", *J. Geophys. Res.*, **112**, D16208, <http://dx.doi.org/10.1029/2007JD008427>.